

June 13, 2007

Scalable nanotemplate assisted directed assembly of single walled carbon nanotubes for nanoscale devices

Prashanth Makaram

Northeastern University - NSF Nanoscale Science and Engineering Center for High-Rate Nanomanufacturing

Sivasubramanian Somu

Northeastern University - NSF Nanoscale Science and Engineering Center for High-Rate Nanomanufacturing

Xugang Xiong

Northeastern University - NSF Nanoscale Science and Engineering Center for High-Rate Nanomanufacturing

Ahmed A. Busnaina

Northeastern University - NSF Nanoscale Science and Engineering Center for High-Rate Nanomanufacturing

Yung-Joon Jung

Northeastern University - NSF Nanoscale Science and Engineering Center for High-Rate Nanomanufacturing

See next page for additional authors

Recommended Citation

Makaram, Prashanth; Somu, Sivasubramanian; Xiong, Xugang; Busnaina, Ahmed A.; Jung, Yung-Joon; and McGruer, Nicol E., "Scalable nanotemplate assisted directed assembly of single walled carbon nanotubes for nanoscale devices" (2007). *Center for High-Rate Nanomanufacturing Publications*. Paper 10. <http://hdl.handle.net/2047/d20000921>

Author(s)

Prashanth Makaram, Sivasubramanian Somu, Xugang Xiong, Ahmed A. Busnaina, Yung-Joon Jung, and Nicol E. McGruer

Scalable nanotemplate assisted directed assembly of single walled carbon nanotubes for nanoscale devices

Prashanth Makaram, Sivasubramanian Somu, Xugang Xiong, Ahmed Busnaina,^{a)}
Yung Joon Jung, and Nick McGruer

NSF Nanoscale Science and Engineering Center for High-Rate Nanomanufacturing, Northeastern University, Boston, Massachusetts 02115

(Received 29 March 2007; accepted 16 May 2007; published online 13 June 2007)

The authors demonstrate precise alignment and controlled assembly of single wall nanotube (SWNT) bundles at a fast rate over large areas by combining electrophoresis and dip coating processes. SWNTs in solution are assembled on prepatterned features that are 80 nm wide and separated by 200 nm. The results show that the direction of substrate withdrawal significantly affects the orientation and alignment of the assembled SWNT bundles. *I-V* characterization is carried out to demonstrate electrical continuity of these assembled SWNT bundles. © 2007 American Institute of Physics. [DOI: 10.1063/1.2747193]

Nanoscale electronics based on carbon nanotubes (CNTs) are smaller and more versatile than conventional complementary metal oxide semiconductor (CMOS) electronics. Various CNT based devices including scanning probes,¹ field emitters,² field effect transistors,³ biological sensors,⁴ chemical sensors,⁵ and memory devices⁶ have been fabricated and studied. For realization of large scale production of single walled nanotube (SWNT) based devices, controlled assembly and precise alignment of SWNTs on prefabricated structures over large areas have been proposed. To achieve this, attempts such as catalytic growth of nanotubes,⁷ self-assembly of nanotubes on chemically modified surfaces,⁸ electric field assisted assembly of nanotubes⁹ on nanostructures, and dip coating have been utilized with partial success. Electrophoresis has been used to assemble SWNTs^{10,11} on prefabricated conductive electrodes. Even though controlled assembly of SWNT can be achieved by electrophoresis, further chemical modifications of SWNTs¹² and/or the substrate¹³ are necessary for orienting these SWNTs in a predetermined direction. Dip coating, a time consuming process, involves immersion of a substrate into a solution containing the material to be coated, followed by gradual withdrawal of the substrate from the solution. While the dip coating method has been employed to assemble and orient DNA (Ref. 14) and carbon nanotubes, patterned chemical functionalization of the substrate¹⁵ is required for controlled assembly. In this letter, we present a SWNT assembly technique using nanotemplate assisted electrophoretic deposition and dip coating processes. This method enables us to construct highly aligned SWNT bundles down to 80 nm in width. These SWNT networks can be directly used as SWNT based interconnect,^{16,17} diverse sensing elements,^{18,19} and other active components^{20,21} in nanoelectronic devices. In addition, our approach is compatible with current CMOS processes and can be easily scaled up for high rate and high volume processing.

A schematic diagram of our assembly technique is depicted in Fig. 1. Electron beam lithography is employed to write nanoscale patterns directly onto a positive tone polym-

ethyl methacrylate (PMMA) resist spun on a gold coated substrate. After exposure the PMMA is developed using a (1:3) methyl isobutyl ketone:isopropyl alcohol (IPA) mixture for 70 s, followed by IPA rinsing for 20 s. This results in the formation of nanoscale patterned trenches in the PMMA film, exposing parts of the gold surface. Arrays of patterned trenches are on $(1.5 \times 1.5 \text{ cm}^2)$ silicon chips, with each array covering an area of $10000 \mu\text{m}^2$. The arrays are composed of several parallel trenches of various widths and pitches defined by e-beam lithography, as described above. This patterned substrate along with a gold reference electrode is immersed into a solution (pH 8) containing dispersed SWNTs. The SWNTs are synthesized using the high pressure carbon monoxide process. The diameter of these SWNTs is between 1 and 2 nm. The ends of the SWNTs in the solution are terminated by carboxylic acid groups and they adsorb ions such as H^+ and OH^- from the solution resulting in a net negative charge on the SWNTs.²² A constant voltage is then

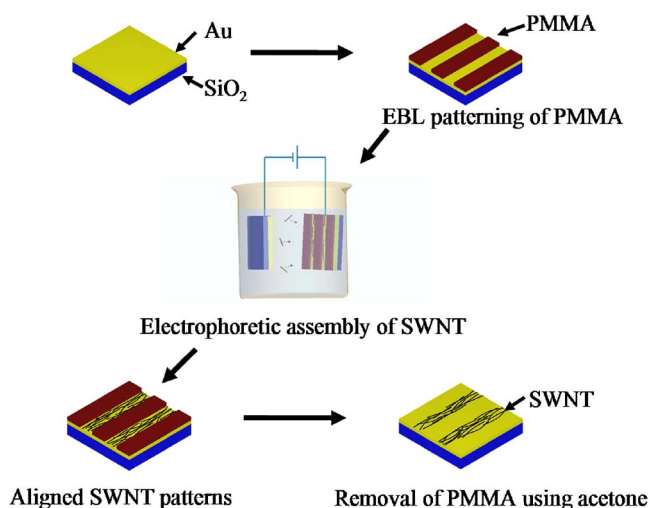


FIG. 1. (Color online) Figure shows a schematic diagram of the assembly process. 200 nm Au is deposited on a SiO₂/Si substrate by sputtering with a 2 nm Cr adhesion layer. 150 nm of positive tone PMMA e-Beam resist is spun on this Au/Cr/SiO₂/Si substrate. e-Beam lithography is then carried out followed by development of the exposed resist. With the nanotemplate being the positive electrode, electrophoresis together with dip coating is carried out. The unexposed PMMA after assembly is removed with acetone.

^{a)} Author to whom correspondence should be addressed; electronic mail: busnaina@coe.neu.edu

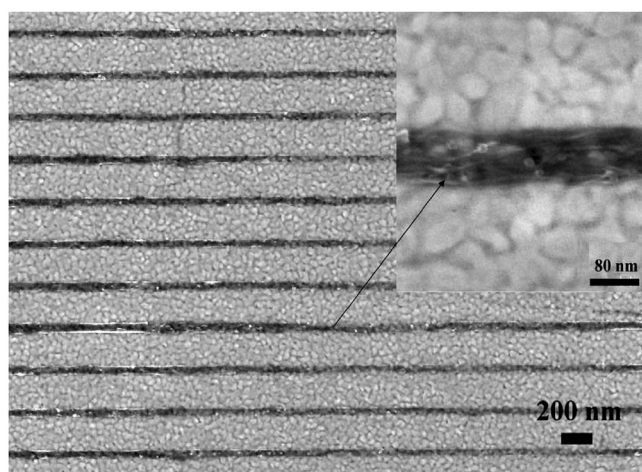


FIG. 2. Figure shows a SEM image of assembled SWNT bundles on gold substrate in a regular array with high control over the orientation. The width of each SWNT bundle is approximately 80 nm and the bundles are separated by 200 nm. The inset is a high resolution image of one of these assembled SWNT bundles.

applied between the substrate and the reference electrode with the substrate being the positive electrode. In the presence of the applied electric field the negatively charged SWNTs migrate toward the substrate and assemble only on areas of gold that are exposed. After 60 s the substrate is drawn out of the solution at a rate of 50 mm/min with the potential still applied. When the substrate is drawn out of the solution the potential is turned off and the PMMA is removed by using acetone followed by IPA. The adhesion of the assembled SWNTs to the hydrophilic gold surface is strong enough that the assembled bundles of SWNTs are not disturbed even when the PMMA is dissolved by acetone.

Figure 2 is a representative result of this process, resulting in a highly controlled large scale site selective assembly and alignment of SWNTs. The inset shows a high resolution image of aligned SWNTs assembled on gold with a bundle width of 80 nm. The applied electrode potential difference was 5 V and the concentration of SWNTs in solution was 0.25 g/l. The orientation of the assembled SWNTs is strongly dependent on the orientation of the PMMA trenches with respect to the direction of substrate withdrawal. This is depicted in Fig. 3. Precise alignment is obtained only when the direction of withdrawal coincides with that of the feature's orientation. Irrespective of the number of PMMA trenches (area of coverage) in a chip we found that for a given applied voltage and concentration of the solution, the time period required for assembly remained the same.

The assembly and orientation of SWNTs can be explained by the following mechanism. For open ended SWNTs the majority of the charges are located at the ends. During electrophoresis, SWNTs migrate toward the PMMA/gold substrate and are anchored to the exposed gold surface at their ends, while the rest of the SWNTs are free to float in the solution. When the substrate is withdrawn from the liquid in the dip coating method, an ultrathin film of the solution is formed²³ due to dewetting. This pushes the SWNTs toward the substrate. As the substrate is slowly pulled out of the solution at a constant velocity, the downwardly dewetting liquid exerts a hydrodynamic drag force¹⁵ on the SWNTs. Also, the upward unidirectional removal of the substrate causes the air-liquid contact line to move across the PMMA/

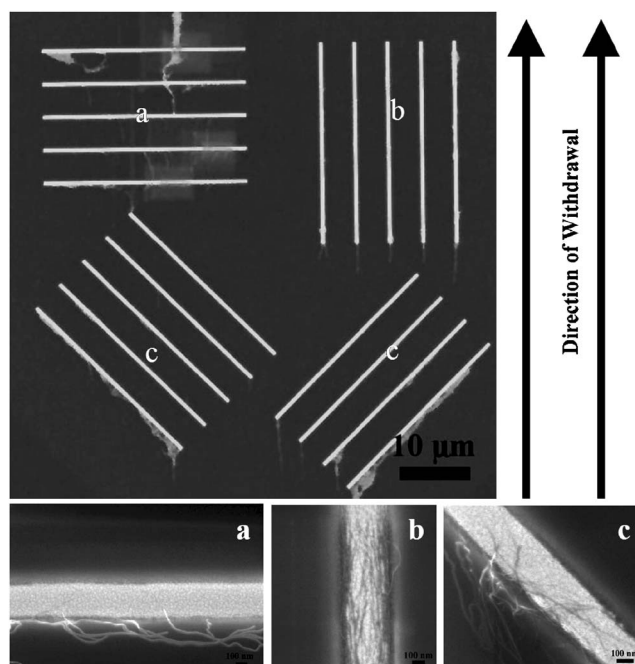


FIG. 3. Effect of orientation of the SWNTs as a function of the angle between the patterns and the direction of withdrawal is depicted in this figure. The nanopatterns are (a) perpendicular, (b) parallel, and (c) at a 45° angle to the direction of substrate withdrawal. It is observed that the orientation by dip coating is effective if and only if the direction of withdrawal is parallel to that of the nanopatterns.

gold substrate exerting a surface tension force on the SWNTs. This surface tension in combination with that of the viscous drag force results in a tensile force acting on the SWNTs that stretches the SWNTs in the direction of the receding liquid. The use of a hydrophobic resist such as PMMA confines the drying of this liquid film to the nanopatterned geometries, thereby organizing the SWNTs into uniform ordered arrays defined by the patterns in PMMA. If the applied potential is turned off during the withdrawal of the substrate from the liquid, the fluidic forces acting on the SWNT is much greater than the SWNT-gold adhesion force resulting in minimal assembly of SWNTs. We observed that the SWNTs do not assemble onto the gold surface when the process is repeated without electrophoresis.

To study the electrical characteristics of the assembled SWNT, after the assembly was performed as described above, we spun PMMA on top of the assembled SWNT/gold layer and patterned the PMMA using e-beam lithography. The e-Beam lithography was carried out in such a way that the unexposed PMMA acted as a mask during the Au/Cr wet etch process defining the necessary contact pads, as shown in Fig. 4(a). All the unmasked Au/Cr areas were removed by the wet etching process, including the Au/Cr underneath the assembled SWNT. Following the wet etching process the unexposed PMMA was removed by acetone. Figure 4(a) shows the second fabrication process steps. Each pair of contact pads is separated by a distance of 800 nm and is connected by several parallel bundles of aligned SWNTs. Top down scanning electron microscopy (SEM) and atomic force microscopy (AFM) images of these assembled SWNTs with electrodes are shown in Figs. 4(b) and 4(c), respectively. A typical *I-V* measurement for five 120 nm wide parallel bundles of assembled SWNT is shown in Fig. 4(d). The calculated average Ohmic resistance is 200 kΩ yielding a resis-

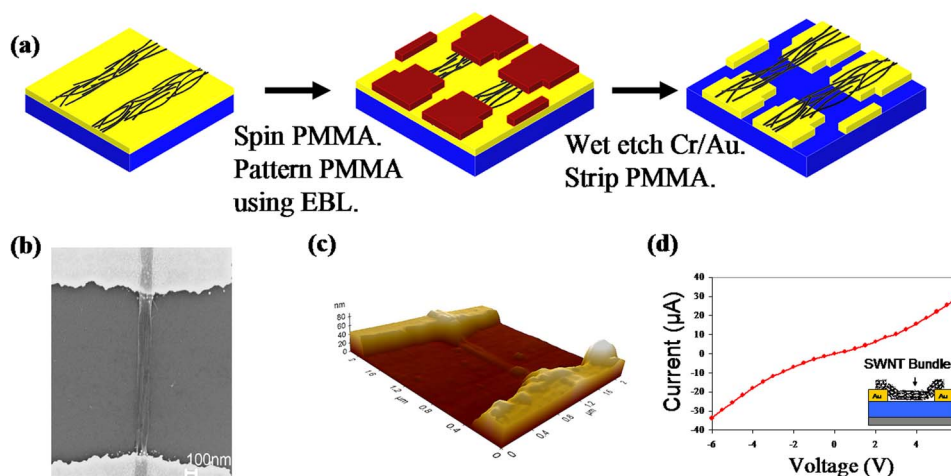


FIG. 4. (Color online) (a) Schematic diagram of the test structure obtained as a result of postfabrication processes after assembly. (b) Top down SEM image of the assembled SWNT bundle with electrodes. (c) AFM image of the assembled SWNT bundle. The height of the assembled SWNT bundle is approximately 15 nm. (d) Typical I - V curve for one of the assembled SWNT bundles. The inset shows a schematic cross section of the test structure.

tance of $1\text{ M}\Omega$ per bundle. Primary contributions to this observed resistance might be the tunneling of charge carriers between SWNTs in the bundle and contact resistance between the SWNT bundles and the electrodes.^{3,20,24,25}

In conclusion we have demonstrated that, by employing both electrophoresis and dip coating, SWNTs suspended in solution can be assembled on prefabricated structures with precise alignment and control over large areas within a short period of time. It is also shown that the direction of substrate withdrawal significantly affects the alignment and orientation of directed assembly of SWNT bundles. These assembled SWNT bundles are shown to exhibit electrical continuity. The time period for assembly is short and hence the scalability of this technique is quite promising. Since our technique involves no chemical modification of the substrate, our process can be easily integrated with current CMOS fabrication processes, resulting in the realization of mass produced SWNT based devices.

¹H. Dai, J. H. Hafner, A. G. Rinzler, D. T. Colbert, and R. E. Smalley, *Nature (London)* **384**, 147 (1996).

²D. S. Y. Hsu and J. Shaw, *Appl. Phys. Lett.* **80**, 118 (2002).

³S. J. Tans, A. R. M. Verschueren, and C. Dekker, *Nature (London)* **393**, 49 (1998).

⁴S. S. Wong, E. Joselevich, A. T. Woolley, C. L. Cheung, and C. M. Lieber, *Nature (London)* **394**, 52 (1998).

⁵G. Overney, W. Zhong, and D. Tomanek, *J. Phys. D* **27**, 93 (1993).

⁶J. W. Ward, M. Meinhold, B. M. Segal, J. Berg, R. Sen, R. Sivarajan, D. K. Brock, and T. Rueckes, *IEEE Non-Volatile Memory Technology Symposium* (IEEE, New York, 2004), p. 34.

⁷J. Kong, H. Soh, A. Cassell, C. F. Quate, and H. Dai, *Nature (London)* **395**, 878 (1998).

⁸Y. Huang, X. Duan, Q. Wei, and C. M. Lieber, *Science* **291**, 630 (2001).

⁹M. Dimaki and P. Boggild, *Phys. Status Solidi A* **203**, 1088 (2006).

¹⁰M. S. Kumar, S. H. Lee, T. Y. Kim, T. H. Kim, S. M. Song, J. W. Yang, K. S. Nahm, and E.-K. Suh, *Solid-State Electron.* **47**, 2075 (2003).

¹¹F. Wakaya, T. Nagai, and K. Gamo, *Microelectron. Eng.* **63**, 27 (2002).

¹²P. V. Kamat, K. G. Thomas, S. Barazzouk, G. Girishkumar, K. Vinodgopal, and D. Meisel, *J. Am. Chem. Soc.* **126**, 10757 (2004).

¹³M. Lee, J. Im, B. Y. Lee, S. Myung, J. Kang, L. Huang, Y.-K. Kwon, and S. Hong, *Nat. Nanotech.* **1**, 66 (2006).

¹⁴C. A. P. Petit and J. D. Carbeck, *Nano Lett.* **3**, 1141 (2003).

¹⁵H. Ko, S. Peleshanko, and V. V. Tsukruk, *J. Phys. Chem. B* **108**, 4385 (2004).

¹⁶P. Pop, D. Mann, J. Reifenberg, K. Goodson, and H. Dai, *Tech. Dig. - Int. Electron Devices Meet.* **2005**, 253.

¹⁷P. M. Albrecht, R. M. Farrell, W. Ye, and J. W. Lyding, *Third IEEE Conference on Nanotechnology* (IEEE, New York, 2003), Vol. 1, p. 327.

¹⁸N. Sinha, J. Ma, and J. T. W. Yeow, *J. Nanosci. Nanotechnol.* **6**, 573 (2006).

¹⁹T. Someya, J. Small, P. Kim, C. Nuckolls, and J. T. Yardley, *Nano Lett.* **3**, 877 (2003).

²⁰R. Martel, T. Schmidt, H. R. Shea, T. Hertel, and Ph. Avouris, *Appl. Phys. Lett.* **73**, 2447 (1998).

²¹L. Liu, C. S. Jayanthi, M. J. Tang, S. Y. Wu, T. W. Tomblor, C. Zhou, L. Alexseyev, J. Kong, and H. Dai, *Phys. Rev. Lett.* **84**, 4950 (2000).

²²H. Hu, A. Yu, E. Kim, B. Zhao, M. E. Itkis, E. Bekyarova, and R. C. Haddon, *J. Phys. Chem. B* **109**, 11520 (2005).

²³A. A. Darhuber, S. M. Troian, J. M. Davis, S. M. Miller, and S. Wagner, *J. Appl. Phys.* **88**, 5119 (2000).

²⁴A. Bachtold, M. Henny, C. Terrier, C. Strunk, C. Schonenberger, J.-P. Salvetat, J.-M. Bonard, and L. Forro, *Appl. Phys. Lett.* **73**, 274 (1998).

²⁵T. W. Ebbesen, H. J. Lezec, H. Hirua, J. W. Bennett, H. F. Ghaemi, and T. Thio, *Nature (London)* **382**, 54 (1996).